

Variability and trends of downward surface global solar radiation over the Iberian Peninsula based on ERA-40 reanalysis

João Carlos Perdigão,^{a*} Rui Salgado,^b Maria João Costa,^b Hari Prasad Dasari^c
and Arturo Sanchez-Lorenzo^d

^a Departamento de Física, Instituto de Ciências da Terra, Instituto de Investigação e Formação Avançada, Universidade de Évora, Portugal

^b Departamento de Física, Instituto de Ciências da Terra, Escola de Ciências e Tecnologia, Universidade de Évora, Portugal

^c Physical Sciences and Engineering Division, King Abdullah University of Science and Technology, Thuwal, Saudi Arabia

^d Instituto Pirenaico de Ecología, Consejo Superior de Investigaciones Científicas (IPE-CSIC), Zaragoza, Spain

ABSTRACT: A climate study of the incidence of downward surface global solar radiation (SSRD) in the Iberian Peninsula (IP) based primarily on ERA-40 reanalysis is presented. NCEP/NCAR reanalysis and ground-based records from several Portuguese and Spanish stations have been also considered. The results show that reanalysis can capture a similar inter-annual variability as compared to ground-based observations, especially on a monthly basis, even though annual ERA-40 (NCEP/NCAR) values tend to underestimate (overestimate) the observations with a mean relative difference of around 20 W m^{-2} (40 W m^{-2}). On the other hand, ground-based measurements in Portuguese stations during the period 1964–1989 show a tendency to decrease until the mid-1970s followed by an increase up to the end of the study period, in line with the dimming/brightening phenomenon reported in the literature. Nevertheless, there are different temporal behaviours as a greater increase since the 1970s is observed in the south and less industrialized regions. Similarly, the ERA-40 reanalysis shows a noticeable decrease until the early 1970s followed by a slight increase up to the end of the 1990s, suggesting a dimming/brightening transition around the early 1970s, earlier in the south and centre and later in the north of the IP. Although there are slight differences in the magnitude of the trends as well as the turning year of the dimming/brightening periods, the decadal changes of ERA-40 fairly agree with the ground-based observations in Portugal and Spain, in contrast to most of the literature for other regions of the world, and is used in the climatology of the SSRD in the study area. NCEP/NCAR reanalysis does not capture the decadal variations of SSRD in the IP. The results show that part of the decadal variability of the global radiation in the IP is related to changes in cloud cover (represented in ERA-40).

KEY WORDS radiation variability; radiation trends; downward surface global solar radiation; total cloud cover; ERA-40; NCEP/NCAR; ground-based observations; Iberian Peninsula

Received 23 April 2015; Revised 11 November 2015; Accepted 13 November 2015

1. Introduction

It is well known that the most important factor that shapes the climate of our planet is the solar radiation that reaches the Earth, so any changes in radiation will induce modifications on temperature, humidity, rainfall, etc. Meanwhile, renewable energies constitute a vital resource for the near future. In particular, solar energy is becoming an increasingly reliable and competitive source of energy, and the correct evaluation of this resource and estimation of its trends, in the present and in the near future, is critical in assessing the viability of projects of solar power plants (e.g., Hammer *et al.*, 2003; Wild *et al.*, 2015).

In recent decades, the scientific community has dedicated some attention to surface solar radiation and to its

variation all over the globe. Some studies reported that between the 1950s and mid-1980s, there was a decrease in the surface solar radiation, a phenomenon known as ‘global dimming’ (Ohmura and Lang, 1989; Stanhill and Moreshet, 1992; Stanhill and Cohen, 2001, among others). Later, the opposite effect was observed, which is known as ‘global brightening’ (e.g. Wild *et al.*, 2005).

During the last few years, many authors have dedicated their attention to the study of surface solar radiation decadal variations over different regions of the globe, such as China (Liu *et al.*, 2010; Xia, 2010; Wang *et al.*, 2015), the Tibetan Plateau (You *et al.*, 2013), Northeast Brazil (Silva *et al.*, 2010), the whole of Europe (Chiaccchio and Wild, 2010; Sanchez-Lorenzo *et al.*, 2015), Northern Europe (Stjern *et al.*, 2009), Southern Europe (Sanchez-Lorenzo *et al.*, 2013a; Mateos *et al.*, 2014; Manara *et al.*, 2015) or the United States (Liepert, 2002; Augustine and Dutton, 2013).

Many attempts to explain these effects have been made, and the major candidates are the changes in the amount

* Correspondence to: J. C. Perdigão, Departamento de Física, Instituto de Ciências da Terra, Instituto de Investigação e Formação Avançada, Universidade de Évora, Rua Romão Ramalho, 59, Évora 7000-671, Portugal. E-mail: perdi.j@gmail.com

and properties of clouds in the atmosphere (Liley, 2009; Russak, 2009; Stjern *et al.*, 2009; Chiacchio *et al.*, 2010; among others) and aerosol concentrations (Norris and Wild, 2007; Sanchez-Lorenzo *et al.*, 2009, among others). For example, Liley (2009) found an increasing trend of cloudiness in New Zealand until the end of the eighties and then an opposite trend, in line with the observed dimming/brightening phenomenon observed in surface solar radiation series. Chiacchio *et al.* (2010) found changes in decadal solar radiation in Alaska and explained the same as a result of changes in clouds and atmospheric circulation patterns over the Pacific. Russak (2009) distinguished two different periods over Estonia between 1950 and 2007 and found correlations between changes in solar radiation and the amount of low clouds as well as the transparency of the atmosphere.

Other studies explain the dimming/brightening periods as the result of the changes in aerosol effects in the atmosphere (e.g., Liepert and Tegen, 2002; Wild *et al.*, 2005; Norris and Wild, 2007) due to their ability to directly and indirectly affect the solar radiation that reaches the surface of the Earth (e.g., Lohmann and Feichter, 2005; Yu *et al.*, 2006). For example, Qian *et al.* (2007) suggested that in China, the increase of aerosols in the period 1960–1980 was the main factor that led to a decrease in solar radiation in clear sky conditions.

On the other hand, studies by Alpert *et al.* (2005) and Alpert and Kishcha (2008) revealed relatively higher rates of solar radiation decrease during the dimming period in urban areas than in rural areas, which was attributed to an impact of urbanization on the trends of surface solar radiation. Nevertheless, a recent study by Wang *et al.* (2015), using 105 pairs of stations with collocated measurements of surface solar radiation, concluded that on a global scale, the dimming period cannot be considered an urban effect. For an extensive analysis on the dimming/brightening subject, see review papers of Wild (2009, 2010, 2012).

Regarding the use of reanalysis products to study the climatology and changes in surface solar radiation, it is worth mentioning that Kaurola *et al.* (2010) stated that ERA-40 data evaluated on a monthly basis reduced the bias on the surface radiation as compared to the records on a daily basis, especially when temporal variations related to cloud radiative effects are studied. Similarly, Betts *et al.* (2006) verified that ERA-40 reproduced the most important variations associated with clouds and shortwave radiation. However, Wild and Schmucki (2011) found that the strong ERA-40-simulated decline in cloud amount over Europe is not observed to the same extent in ground-based records and that the reanalysis product fails to reproduce the dimming/brightening phenomenon. Träger-Chatterjee *et al.* (2010) assessed the downward surface solar irradiation for Germany from reanalysis products and found some limitation to the adequate representation of the clouds, especially in summer. However, reanalysis products have some advantages over historically observed series as a variety of meteorological data obtained by different instrumentation (surface observations, satellites, aircraft, etc.) is assimilated, allowing a consistency in the data obtained by

the quality control of the model while presenting a regular spatial and temporal resolution.

The North Atlantic Oscillation (NAO) is a major phenomenon that influences the weather and climate variability of Europe (Hurrell, 1995, 1996). The NAO is related to precipitation (Hurrell, 1995; Trigo *et al.*, 2002) and influences the temporal and spatial variability in the Iberian Peninsula (IP). Specifically, the positive (negative) phase of the NAO explains a reduction (increase) of precipitation and a decrease (increase) in the percentage of cloud fraction over the south of Europe. In Portugal, high values in the NAO index correlate with low values of precipitation and cloudiness (Trigo *et al.*, 2002). Sanchez-Lorenzo *et al.* (2009) described that cloud cover and sunshine duration over the IP are linked to the NAO, especially during winter. Pozo-Vázquez *et al.* (2004) found high correlations between the NAO index and the monthly sums of sunshine duration for the IP.

Sanchez-Lorenzo *et al.* (2009) stated that clouds show a decreasing trend in the IP between 1960 and the middle of 2000, whereas sunshine duration series shows a decrease from the 1950s to the mid-1980s (dimming), with a subsequent increase until the 2000s (brightening). Sanchez-Lorenzo *et al.* (2013a) found a positive trend for global radiation in the 1985–2010 period with a value of $+3.9 \text{ W m}^{-2}$ per decade, in line with the sunshine duration trends since the 1980s, from the analysis of 13 Spanish observational stations. Mateos *et al.* (2014) found a strong brightening in the IP for the period 2003–2012 as a result of a decrease of clouds and aerosols in the region. Seventy-five percent of the decreasing trends observed for shortwave radiation was explained as being caused by clouds and the remaining 25% by the effect of aerosols.

The main objective of this work is to study the patterns, evolution and trends of downward surface global solar radiation at the surface of the IP with ERA-40 reanalysis data and explore its relationship with clouds. Section 2 presents the data, the study area and describes the methodology used for this study; in Section 3, shortwave radiation reanalysis data were compared to the measurements taken during the common period at Portuguese and Spanish meteorological stations. In Section 4, annual and monthly area-averaged values of downward surface global solar radiation and total cloud fraction are computed for the ERA-40 reanalysis product and analysed for the IP region. Temporal averages of shortwave radiation and total cloud cover (TCC) were carried out over the entire ERA-40 period. Finally, conclusions are presented in Section 5.

2. Data and methods

2.1. Data and area of study

The daily downward surface global solar radiation (SSRD, in W m^{-2}) data measured at Portuguese meteorological stations (Bragança, Porto, Évora and Faro) were obtained from the World Radiation Data Centre (WRDC, <http://wrdc-mgo.nrel.gov/>). SSRD from other Portuguese stations, also available at the WRDC was not considered

Table 1. Location and data availability for the Portuguese stations.

Station	Period	Latitude (N)	Longitude (W)	Altitude (m)	Missing monthly data (%)
Lisbon	1958–1989	38.43	−9° .09	77	0
Monte Estoril	1964–1989	38.42	−9.24	31	90.7
Porto	1964–1989	41.08	−8.36	93	2.2
Coimbra	1964–1989	40.12	−8.25	141	10
Faro	1964–1986	37.01	−7.58	7	0.4
Évora	1964–1989	38.34	−7.54	309	1.0
Penhas Douradas	1964–1989	40.25	−7.33	1380	19
Castelo Branco	1964–1989	39.50	−7.29	386	82.4
Bragança	1964–1989	41.48	−6.44	691	4.8

Bold stations refer to stations used in this study.

for this study due to insufficient data (Table 1). For Lisbon, the monthly data were obtained directly from the Portuguese Institute of Ocean and Atmosphere (IPMA).

The analysis was done on a monthly mean basis obtained from the daily values. A month was considered only if the data available corresponded to at least two-thirds of that month. In the absence of data for a month at a given station and a given year, the average of all corresponding months in the series was used. The annual average was calculated taking into account those values. The percentage of missing monthly values in the period under study is indicated in Table 1, which also contains the locations of the stations used. In addition, a collection of 13 Spanish series available since 1985 were considered in this study. For more details about the dataset, we refer to Sanchez-Lorenzo *et al.* (2013a).

SSRD and TCC variables from ERA-40 and NCEP/NCAR reanalysis are also used in this study on an annual and seasonal basis. ERA-40 is the 45-year, second generation reanalysis based on the European Centre for Medium-Range Weather Forecast’s (ECMWF) operational, three-dimensional variation assimilation system, making comprehensive use of satellite data and conventional observations (Uppala *et al.*, 2005). It covers the period from September 1957 to August 2002, and the model uses 60 vertical levels and a T159 spectral resolution. The shortwave radiative variables were computed by the Fouquart and Bonnel (1980) scheme. The data were extracted from the ECMWF portal. The spatial resolution used in the present study is 0.25 × 0.25° every 6 h. NCEP/NCAR data (Kalnay *et al.*, 1996) covers the period from 1948 until the present and has a horizontal resolution of 2.5° × 2.5° (T62 Gaussian grid ~209 km), with 17 pressure levels and 28 sigma levels. Monthly mean data was downloaded from the National Oceanic and Atmospheric Administration (NOAA) portal.

In Section 4, annual and monthly averaged trends for SSRD and TCC are computed from ERA-40 for the IP region (36°–44°N; 10°W–4°E) and for the period from 1958 to 2001. The seasons are defined according to the World Meteorological Organization’s (WMO) nomenclature i.e., winter [December–January–February (DJF)], spring [March–April–May (MAM)], summer [June–

July–August (JJA)] and autumn [September–October–November (SON)].

2.2. Homogenization methods

Climatological series sometimes contain temporal inhomogeneities. In this study, the Standard Normal Homogeneity Test (SNHT, Alexandersson, 1986), Buishand Range Test (Buishand, 1982), Pettitt Test (Pettitt, 1979) and Von Neumann Ratio Test (Von Neumann, 1941) were used to test the homogeneity of the Portuguese series. The absolute homogeneity tests were applied for each station separately (Wijngaard *et al.*, 2003; Morozova and Valente, 2012; Hakuba *et al.*, 2013) as observational stations have a low density (only five) and are considerably spaced from each other. The Pettitt Test, SNHT and Buishand test specifically suppose that tested values are independent and are normal distributed identically (null hypothesis), while under alternative hypothesis, the tests assume inhomogeneous series as a consequence of a break or a shift. On the other hand, for the Von Neumann Ratio Test, the null hypothesis is that the data are independent and identically distributed random values and with the alternative hypothesis, that the values in the series are not randomly distributed.

For each of the test’s description, let *n* be the length of a time series to be tested, where *x_i* is *i*-th element of the series with mean *μ* and standard deviation *σ*.

Statistic *T(k)* in the SNHT test compares the mean of the first *k* observations with the mean of the last (*n* − *k*) observations,

$$T(k) = k \left[\frac{1}{k} \sum_{i=1}^k \frac{x_i - \mu}{\sigma} \right]^2 + (n - k) \left[\frac{1}{(n - k)} \sum_{i=k+1}^n \frac{x_i - \mu}{\sigma} \right]^2, \quad k = 1, \dots, n \tag{1}$$

The null hypothesis is rejected if *T₀* = max_{1 ≤ k ≤ n} *T(k)* and if *T₀* is above a certain level given in a table of Khaliq and Ouarda (2007).

The Buishand statistic test, *S(k)*, is defined as

$$S(k) = \sum_{i=1}^k (x_i - \mu), \quad k = 1, \dots, n \tag{2}$$

with *S(0)* = 0 and R statistic given by

$$R = \left(\max_{0 \leq k \leq n} S(k) - \min_{0 \leq k \leq n} S(k) \right) / \sigma \tag{3}$$

Critical values for *R*/√*n* were obtained from Buishand (1982).

Y(k) statistic test for the Pettitt test is calculated as

$$Y(k) = 2 \sum_{i=1}^k r_i - k(n + 1), \quad k = 1, \dots, n \tag{4}$$

As the Pettitt test is a nonparametric test, *r₁* *r_n* is the rank of the *x₁* *x_n*. The critical value of the test *Y(k)* is calculated for a probability level *α* as

$$Y_{k\alpha} = \sqrt{-\ln \alpha (n^3 + n^2) / 6} \tag{5}$$

and a change point occurs when $Y_k = \max_{1 \leq k \leq n} |Y(k)|$.

The Von Neumann ratio test is defined as

$$N = \frac{\sum_{i=1}^{n-1} (x_i - x_{i+1})^2}{\sum_{i=1}^n (x_i - \mu)^2} \tag{6}$$

Critical values with a probability level α were calculated as

$$N_\alpha \sim 2 - 2u_\alpha \sqrt{\frac{n-2}{(n-1)(n+1)}} \tag{7}$$

According to Wijngaard *et al.* (2003) and Hakuba *et al.* (2013), three classes were considered: Class I: useful – one or zero test rejects the null hypothesis; Class II: doubtful – two tests reject the null hypothesis; Class III: suspect – three or four tests reject the null hypothesis. In this work, the null hypothesis was rejected at 1% level. The series in Class I and II may be considered homogeneous whereas inhomogeneous for Class III (Wijngaard *et al.*, 2003).

2.3. Statistical methods

The parameters used to evaluate the data model and meteorological data were the mean, bias (Bias), root mean square error (RMSE), the correlation coefficient (r) and coefficient of variation (CV). For a series with x_i values, with mean (μ) and standard deviation (σ), the CV (in percentage) is defined as:

$$CV (\%) = \frac{\sigma}{|\mu|} \times 100 \tag{8}$$

This parameter measures the variability in the values of a series relative to its mean.

Normalized Bias, in percentage, is defined as:

$$NBIAS (\%) = \frac{BIAS}{\frac{1}{n} \sum_{i=1}^n x_i} \times 100 \tag{9}$$

A simple linear regression model (including the determination coefficient – R^2) as well the nonparametric statistical method of Mann–Kendall (Mann, 1945) were applied to find possible trends in annual and monthly data. The method of Mann–Kendall (MK test) has been widely used by several authors in meteorological studies (Cislaghi *et al.*, 2005; Obot *et al.*, 2010; Silva *et al.*, 2010, among others) to statistically assess if there is a monotonic upward or downward trend of the variable of interest over time, and it is recommended by the WMO.

Specifically, for a time series containing a set of observations (x_1, \dots, x_n), the MK test is given by

$$S = \sum_{i=1}^{n-1} \sum_{j=i+1}^n \text{sign}(x_i - x_j) \tag{10}$$

where

$$\text{sign}(x_i - x_j) = 1 \text{ if } (x_i - x_j) > 0$$

$$\text{sign}(x_i - x_j) = -1 \text{ if } (x_i - x_j) < 0 \tag{11}$$

$$\text{sign}(x_i - x_j) = 0 \text{ if } (x_i - x_j) = 0$$

The statistical value of the test is the Mann–Kendall index (Z_{MK}), given by

$$Z_{MK} = \begin{cases} \frac{S-1}{\sigma} & \text{if } S > 0 \\ 0 & \text{if } S = 0 \\ \frac{S+1}{\sigma} & \text{if } S < 0 \end{cases} \tag{12}$$

with

$$\sigma = \sqrt{\frac{1}{18} \left[n(n-1)(2n-5) - \sum_{p=1}^q t_p(t_p-1)(2t_p+5) \right]} \tag{13}$$

A positive value in Equation (10) indicates that there is a positive trend in the observations, and a very large value of S reveals that the latest observations correspond to higher values than the first for the same series; on the other hand, if the result of Equation (10) gives a negative value, it can be assumed that there is a negative trend. In the present study, a α level of 5% is considered significant, which corresponds to $|Z_{MK}| \geq 1.96$. The α level value is obtained from the standard normal distribution table.

The sequential version of the MK test (with the acquisition of two series – one regressive and another progressive), slightly modified by Sneyers (1975), allows to determine the point in time when the trend starts and when it becomes meaningful. In this version of the MK test, original values of a set of observations (x_1, \dots, x_n) are replaced by their ranks y_i in ascending order. The magnitude of $y_i, (i = 1, \dots, N)$ are compared with $y_j, (i = 1, \dots, N)$, and a statistic test is defined as

$$t_i = \sum_{j=1}^i n_j \tag{14}$$

where n_i represents the sum of a temporal series whose values $y_i > y_j$. Assuming that there is a trend (null hypothesis is rejected), the series presents a normal distribution and variance given by

$$E(t_n) = \frac{n(n-1)}{4} \tag{15}$$

$$\text{VAR}(t_n) = \frac{n(n-1)(2n+5)}{72} \tag{16}$$

The sequential values of the statistic are given by

$$u(t_n) = \frac{(t_n - E(t_n))}{\sqrt{\text{VAR}(t_n)}} \tag{17}$$

The progressive series (forward direction) is determined from Equation (17), starting from the value $i = 1, \dots, N$ generating the statistical $u(t_n)$. The regressive series is determined backwards from the last term of the series $i = N, \dots, i$, generating the statistical $u'(t_n)$. The

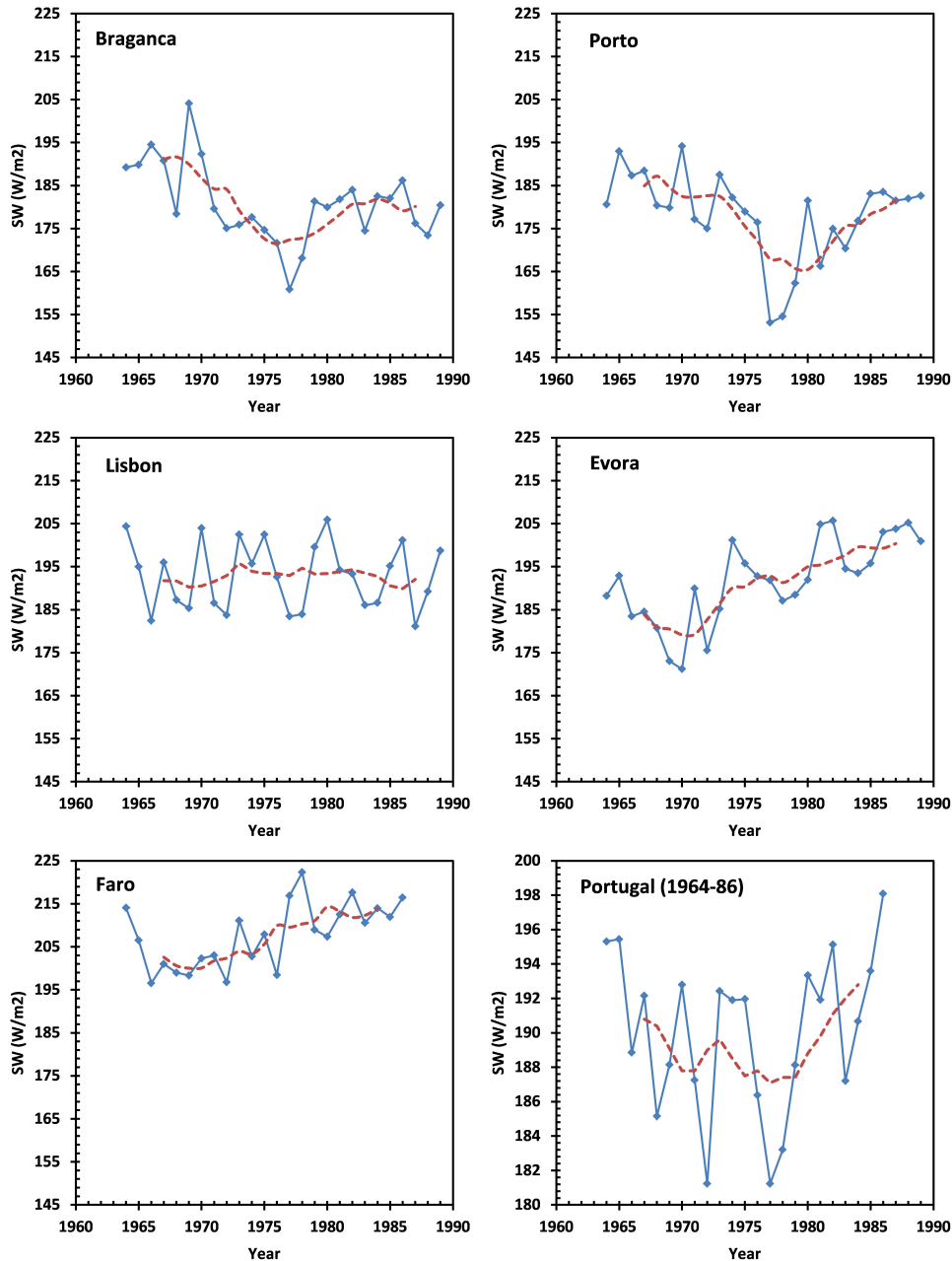


Figure 1. Mean annual global incident radiation observed in Portuguese stations. In the bottom right plot, a mean of five Portuguese series is represented. The red dashed line corresponds to a five-year-centred moving average.

intersection between the progressive $u(t_n)$ and regressive $u'(t_n)$ series should occur within the confidence intervals (CIs), representing the beginning of the trend. The series became significant when the values of statistical data exceed the CIs of 95%.

3. Comparison of shortwave radiation data from ground-based and reanalysis datasets in Portugal and Spain

3.1. Changes of shortwave radiation in ground-based observations of Portugal

Due to the lack of studies dealing with the decadal changes of SSRD over Portugal using ground-based measurements

(e.g., see Sanchez-Lorenzo *et al.*, 2015), in this section, we first introduce their main characteristics. For more details about decadal changes in Spain, we refer to Sanchez-Lorenzo *et al.* (2013a).

As detailed in Section 2.2, the annual SSRD series for Portuguese stations were tested by means of four homogeneity tests. The results confirm that the five series can be considered homogeneous. The Bragança, Porto and Lisboa series specifically obtained a classification of Class I, whereas Évora and Faro were classified as Class II as the null hypothesis was not rejected for the Buishand and Von Neumann tests. Consequently, we have used the five series for the subsequent analyses. Figure 1 shows the mean annual SSRD series in the five observational stations

Table 2. Annual climatology for meteorological stations in Portugal with mean (\bar{X}), standard deviation (σ), slope (b), coefficient of determination (R^2) and MK indice (Z_{MK}) with a α level of confidence of 5%.

Stations	Period	\bar{X}	σ	b	R^2	Z_{MK}
Bragança	1964–1989	181.0	9.0	-0.5	0.2	-1.5
Porto	1964–1989	178.2	10.1	-0.4	0.1	-1.1
Lisbon	1964–1989	192.5	7.8	-0.1	0.0	-0.3
Évora	1964–1989	191.6	9.8	0.9	0.5	3.7
Faro	1964–1986	207.7	7.5	0.7	0.4	2.9

Bold values mean significant trends.

of Portugal. As can be seen from Table 1, the length of time series varies from station to station. In order to smooth the data and facilitate trend detection and qualitative analysis, a five-year-centred moving average was applied. Table 2 shows the climatological parameters on an annual basis for the five Portuguese stations under analysis.

The Porto series clearly shows a decrease of the SSRD by the end of the 1970s with a maximum annual average value of 194 W m^{-2} observed in 1970 and a minimum of 153 W m^{-2} in 1977. Similarly, Bragança reveals a decrease of radiation until the mid-1970s followed by an increase. The maximum annual value was reached in 1969 (204 W m^{-2}) and the minimum value in 1977 (161 W m^{-2}). Évora and Faro present a similar behaviour, contrasting that observed in Porto and Bragança, that is, an increase of SSRD is observed since the early 1970s without any visible dimming period. Regarding Faro, the maximum annual value was registered in 1978 (222 W m^{-2}) and the minimum in 1966, with an average value of 196 W m^{-2} . The Évora station recorded a maximum mean annual value of 205 W m^{-2} in 1982 and a minimum annual value of 171 W m^{-2} in 1970. Finally, in Lisbon, there are no relevant decadal variations in the series, which is in contrast with the changes observed in the other stations in Portugal.

Nevertheless, it is worth mentioning that the use of individual series is questionable, especially when the homogeneity testing of the series has been subjected to absolute methods due to the lack of reference series. For this reason, we have also computed the composite mean series of Portugal (Figure 1) that allows a higher signal-to-noise ratio, enabling a better identification of decadal variations than single station series and reducing the possible inhomogeneities remaining in the series. The SSRD mean values over Portugal range between $\sim 180 \text{ W m}^{-2}$ and $\sim 200 \text{ W m}^{-2}$. It is possible to identify two periods; until the end of the 1970s, the behaviour of the SSRD is characterized by a decrease followed by an increase, in line with previous literature (e.g., Wild, 2009, 2012), although with an earlier turning year as compared to other regions of Europe (e.g., Wild, 2009; Sanchez-Lorenzo *et al.*, 2013b; Sanchez-Lorenzo *et al.*, 2015).

Figure 2 shows the standard deviation of the global radiation on a monthly basis (between the same months) during the period of analysis. In general and in all months, the highest values of variability correspond to the cities of Porto and Bragança (in the north of Portugal), which

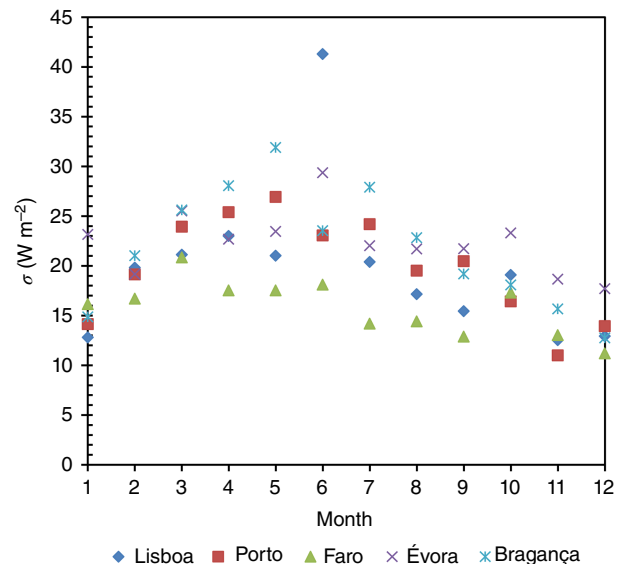


Figure 2. Standard deviations of the observed SSRD monthly means.

in June presents the largest deviation. The inter-annual variability is greater in the cities of Évora and Porto with annual standard deviations of 10 W m^{-2} . The Faro station shows the lowest inter-annual value of 8 W m^{-2} and has the maximum mean value of the SSRD. The observed variability in the SSRD may be associated to inter-annual variability in cloudiness due to atmospheric circulation patterns such as the NAO (Trigo *et al.*, 2002). On the other hand, due to the proximity of the IP to the north of Africa, it is expected that the SSRD is strongly affected by Saharan dust aerosol, particularly in the spring and summer months, as well as by summer forest fires. Saharan dust aerosols increase the aerosol optical depth of the atmosphere and lead to a significant decrease of the solar radiation that reaches the ground (Antón *et al.*, 2012; Valenzuela *et al.*, 2012; Obregón *et al.*, 2015).

Lisbon and Porto are the major Portuguese cities and are located near the coast where the majority of the Portuguese population and industries are concentrated. At the south of Tagus river, the industrialization is less relevant (location of districts of Évora and Faro). An analysis of the population in Portugal shows that in the period under review (1960–1990), the population grew in Lisbon (+53.8%), Porto (+40.5%) and Faro (+8.3%) and decreased in the Évora (-20.7%) and Bragança (-20.8%) districts (Cravidão and Matos, 1990).

The SSRD pattern observed in Bragança and Porto (Figure 1) shows a decrease of SSRD that may be associated to the period commonly known as global dimming (Stanhill and Cohen, 2001). Still, the data shows that the increase in the SSRD appears relatively earlier than that described in the literature, (e.g. Wild *et al.*, 2005; Wild, 2009, 2012). Results seem to indicate that the locations where the industrial topography and demography of the region are relevant are those where the increase of the SSRD arises later or is not visible at all (like in Lisbon). In the remaining stations of Portugal, located in the countryside in the south, with a lower industrial and

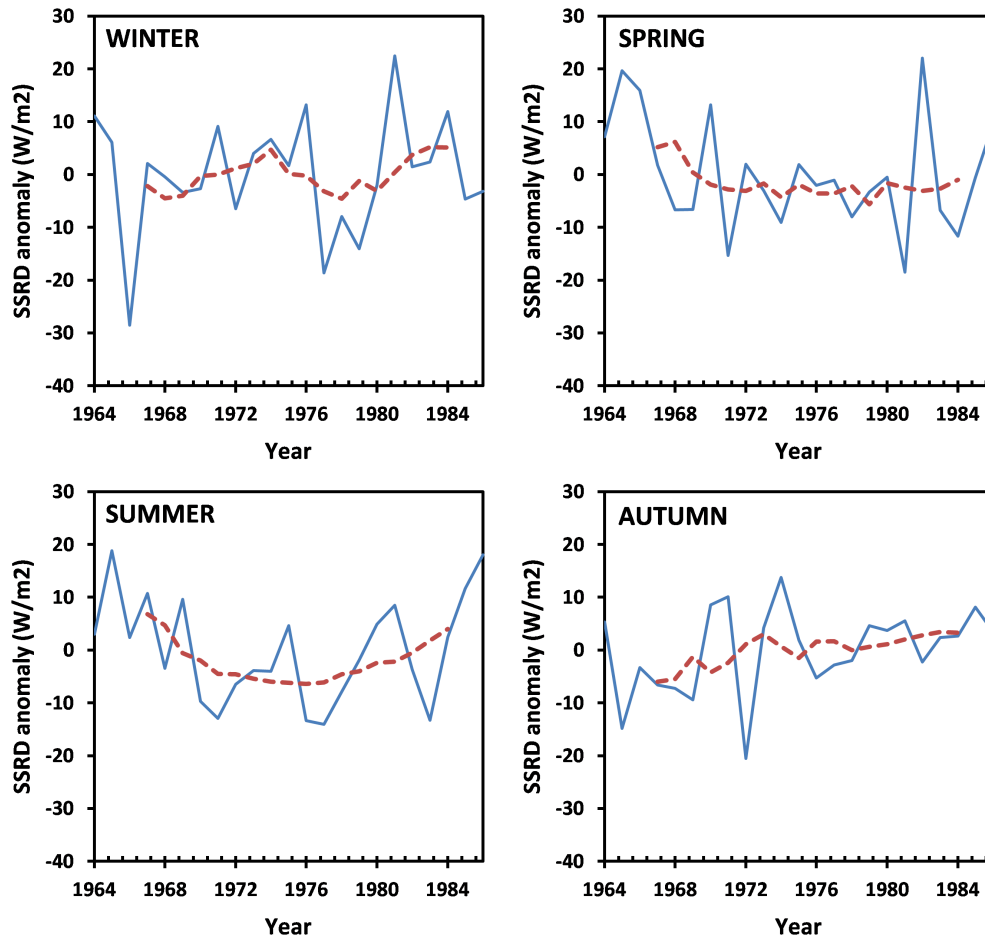


Figure 3. Evolution of seasonal mean SSRD in Portugal in the period 1964–86 (blue solid line). A five year centred moving average was applied (dashed line). Series expressed in anomalies (observation minus mean of reference period).

population density and almost flat topography, the measurements hint at an earlier increase of radiation.

The Évora and Faro stations (cities at south of Portugal) specifically seem to indicate an increase of the SSRD over the whole study period. These cities are located in regions with small industrial density and demographic growth and with only a few occurrences of forest fires when compared with northern Portuguese regions (Leite *et al.*, 2014). Therefore, it is reasonable to assume that the typical atmosphere was characterized by low aerosol loads (background atmospheric aerosol) with occasional events of desert dust or forest fire particle transports, which means that the area did not possibly experience enough aerosol influence to be part of the dimming phenomenon (Alpert and Kishcha, 2008).

Since the area in question had little industrial growth and the dominant circulation brings air masses from the Atlantic Ocean, it does not seem that the concentration of strongly absorbing aerosols (from local areas or from another region) has increased significantly and triggered a pronounced indirect effect of aerosols (as described for example in Twomey *et al.*, 1984 and Albrecht, 1989). Daily 120-h back-trajectory analyses of air masses for the south-western IP, from 2005 to 2010, showed that the most frequent situations observed were the clean and

Table 3. Seasonal linear trends for the SSRD mean over Portugal for different periods.

	Period		
	1964–1986	1964–1977	1978–1986
DJF	0.1	0.0	0.9
MAM	-0.4	-1.2 (80%)	1.1
JJA	-0.0	-1.6 (98%)	1.9 (80%)
SON	0.4 (80%)	0.5	0.5

Trend values in $W m^{-2} year^{-1}$. In parenthesis is presented the α level of confidence obtained by the MK test. Bold value means significant trend and the values in parenthesis indicate the level of significance.

maritime situations (Obregón *et al.*, 2012). This would, at least partly, explain the behavior of the Évora and Faro series, which show a stronger increase of the SSRD than the other Portuguese stations.

Overall, the turning year from the period of decrease and increase of the SSRD was around five years ahead in the stations in the south as compared to the stations in the north (especially Porto station). Results from winter and summer seasons confirm that the beginning of the brightening period was noticed over Portugal in the late seventies. The SSRD in spring and autumn show an opposite

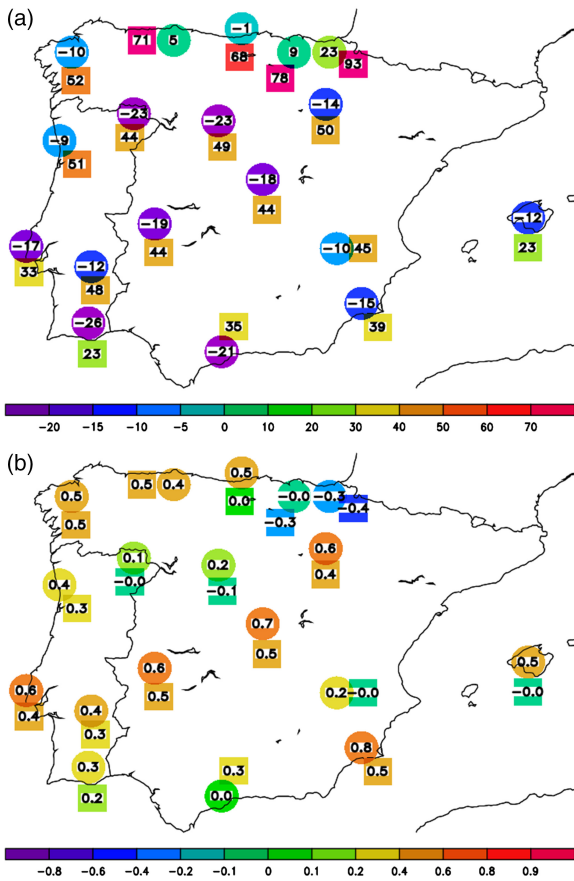


Figure 4. Annual spatial distribution of Bias (a) and correlation coefficient (b) for Portuguese (1964–1986) and Spanish (1985–2001) stations. Squares represent values from validation between NCEP/NCAR and observation data and filled circles results from ERA-40 and observations. Bias values in $W m^{-2}$.

behavior, that is, autumn presents a positive trend without a decrease of the SSRD, and spring season shows a negative trend without an increase (Figure 3). Table 3 contains the seasonal trends over the periods for the mean of five series (Portugal). The linear trend in the majority

of the seasons over Portugal is non-significant over the entire period. The dimming and the brightening trends are mainly observed during summer with $-1.6 W m^{-2} year^{-1}$ and $1.9 W m^{-2} year^{-1}$, respectively. However, the highest level of confidence is only obtained for the observed dimming period.

3.2. Evaluation of ERA-40 and NCEP/NCAR reanalysis products against ground-based measurements

The mean annual cycle and inter-annual variability of ERA-40 and NCEP/NCAR SSRD are compared with the global radiation measured at the meteorological stations described in Section 2. For the analysis, the nearest grid points of the reanalysis products are considered. It is worth noting that the comparisons present some limitations due to the large spatial scale between grid point of reanalysis and observations (e.g., Hakuba *et al.*, 2014). The mean correlation coefficients and the bias values for Portugal and Spain, on an annual and monthly basis, are shown in Figures 4 and Figure 5, respectively, whereas in the Supplementary Material, additional results for individual stations are presented (Figure S1 and Table S1).

ERA-40 (NCEP/NCAR) annual and monthly averaged SSRD radiation values are always lower (higher) than the corresponding ground-based measurement values as indicated by the negative (positive) Bias (Table S1 and Figures 4 and 5). The spatial distribution over the IP (Figure 4) shows a tendency towards negative biases, except in the northern areas, with a better performance of ERA-40 than NCEP reanalysis data. For instance, the ERA-40 database underestimates the SSRD in comparison to the observations with a mean Bias of around $20 W m^{-2}$ (or 10% in relative values) for Portugal, where NCEP/NCAR overestimation is around $40 W m^{-2}$ (or 20% in relative values). It is known (Wild, 2001) that NCEP reanalysis, relative to surface solar radiation, is too transparent, and this is probably one of the reasons that may explain the highest bias found relative to ERA-40.

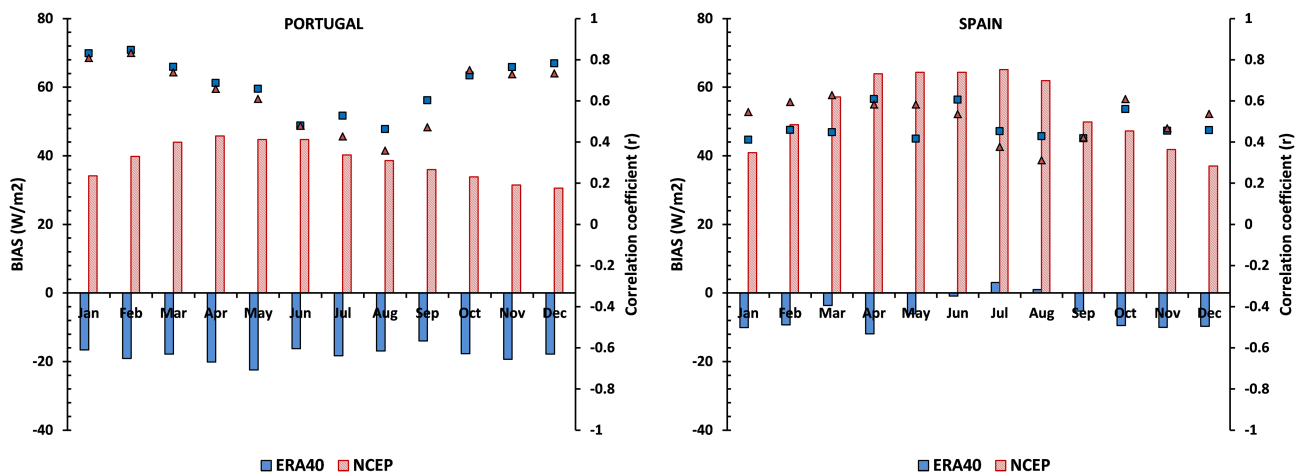


Figure 5. Mean correlation coefficients (triangles for NCEP and squares for ERA-40) and bias (bars) for all stations in Portugal and Spain, between the monthly mean series of observed solar radiation at selected meteorological stations and simulated solar radiation at the nearest grid point of reanalysis product.

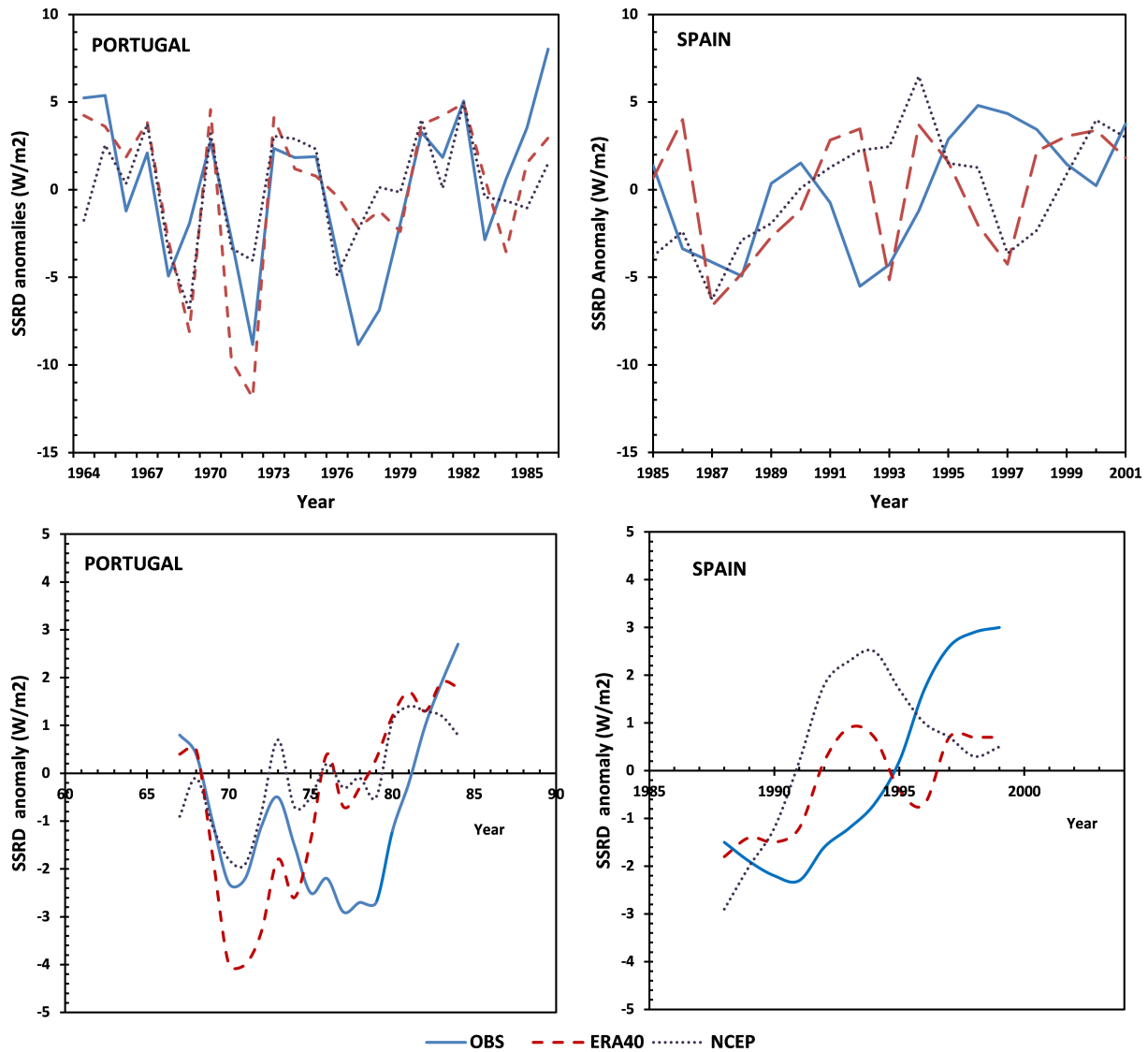


Figure 6. Anomaly mean of annual SSRD for Portugal (1964–86) and Spain (1985–2001) from observations (thick line), ERA-40 (dashed line) and NCEP (dotted line) data. Bottom plots show five years centred moving averaged applied to Portugal and Spain data.

The correlation coefficient (r), on an annual basis (Figure 4), between the data measured at the selected stations and reanalysis products is relatively low, with mean values of $r=0.4$ (ERA-40) and $r=0.2$ (NCEP/NCAR). Spatial distribution of the correlation coefficient is, for both reanalysis, the worst at northern stations either in Portugal or in Spain. It is well known that clouds are structures of various dimensions. Due to the coarse spatial resolution of the reanalysis, cloud properties are not well represented (Kaurola *et al.*, 2010), which may explain, at least partially, the biases, as also found by Träger-Chatterjee *et al.* (2010) in Germany and You *et al.* (2013) in the Tibetan Plateau, especially for the NCEP/NCAR reanalysis.

The reliability of ERA-40 and NCEP/NCAR data to assess the SSRD was also investigated on a monthly basis (Figure 5). In the majority of the months, the values of the correlation coefficient are approximately above 0.6 for Portugal and Spain, indicating a good correlation

Table 4. Linear trends for the annual mean SSRD over three periods in Portugal for observations, ERA-40 and NCEP data.

	Portugal			Spain
	1964–1986	1964–1977	1978–1986	1985–2001
OBS	0.1	–0.5 (90%)	1.1 (90%)	0.4 (90%)
ERA-40	0.1	–0.3 (80%)	0.2	0.2
NCEP/NCAR	0.1	–0.1	–0.1	0.4 (98%)

All values in $W m^{-2} year^{-1}$. In parenthesis is presented the α level of confidence obtained by the MK test. Bold value means significant trend and the values in parenthesis indicate the level of significance.

(see Figure S1). The lowest correlations were obtained for the summer months. In those months, the variance in the observations is much larger than in the reanalysis database probably due to the non-inclusion of the actual concentration of aerosols in the reanalysis process. For instance, the radiative fields of ERA-40 use a climatological aerosol profile and do not take into account the actual aerosol

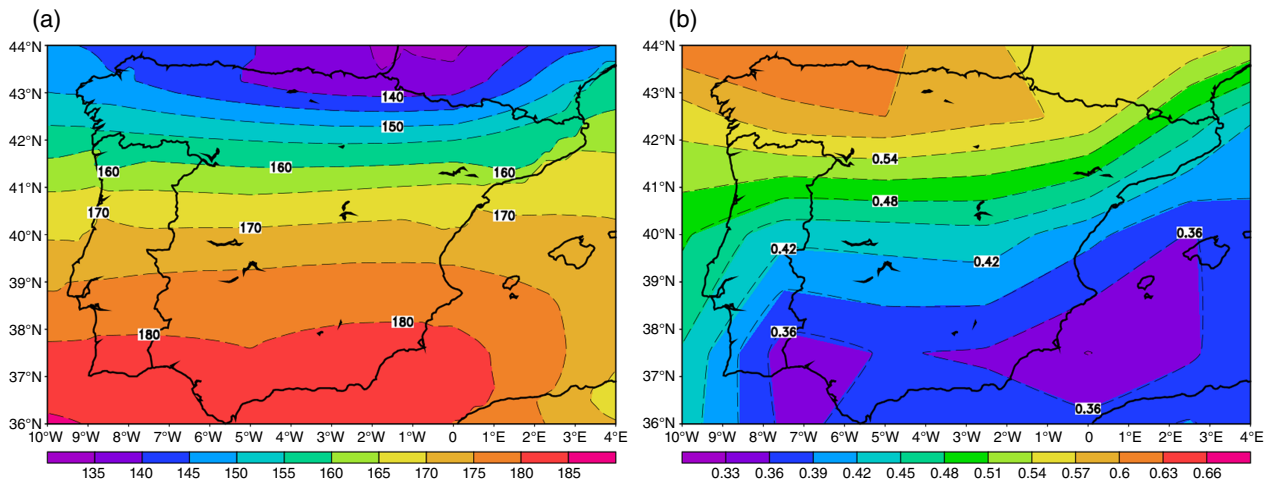


Figure 7. Mean values of the SSRD (a) and TCC (b) from ERA-40. Radiation is expressed in $W m^{-2}$.

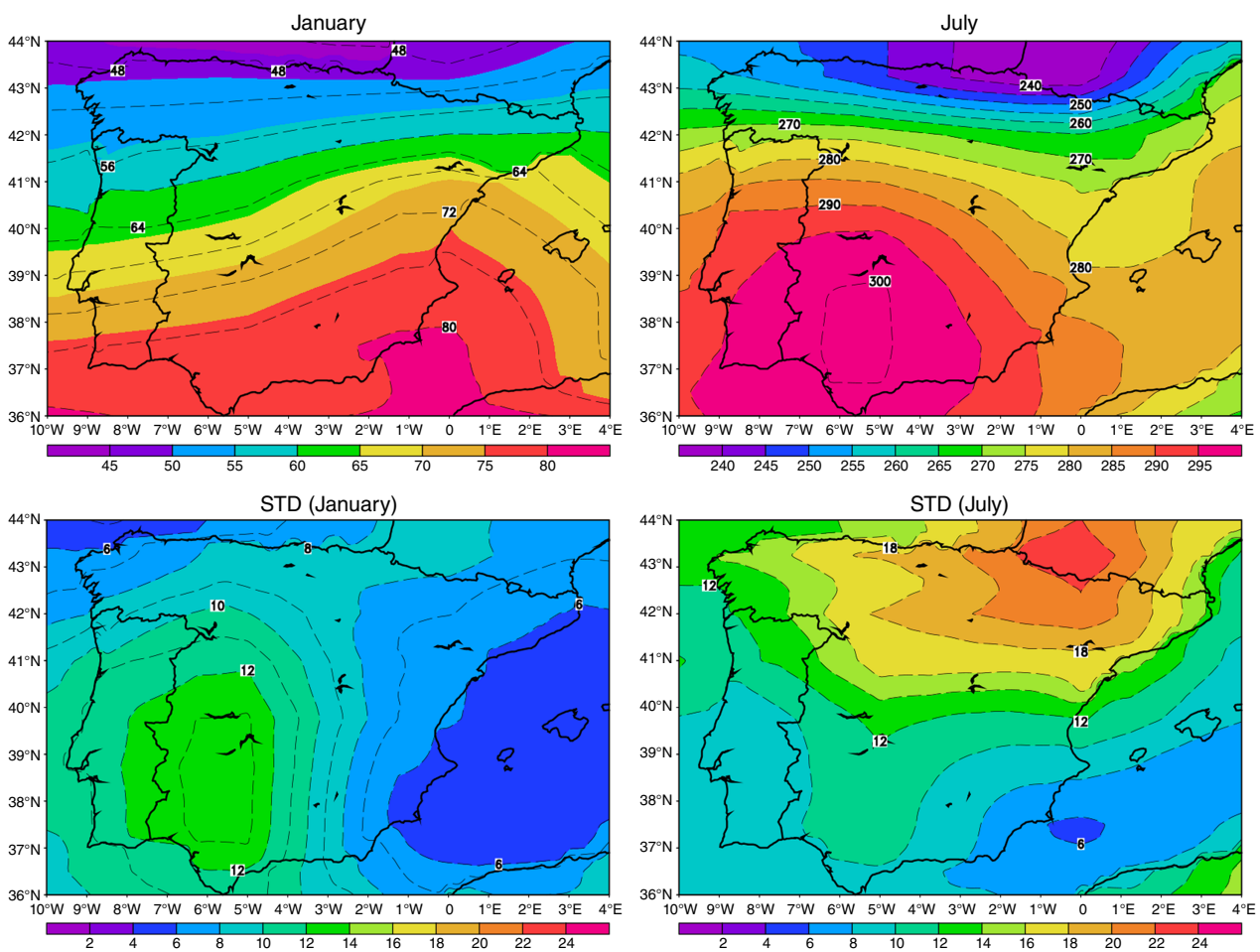


Figure 8. The mean ERA-40 SSRD for January and July and corresponding standard deviation.

type and load (Uppala *et al.*, 2005). Thus, the decrease in the correlations during summertime can be explained by the fact that it is the season with the highest atmospheric aerosol loading over the IP (Alados-Arboledas *et al.*, 2003; Toledano *et al.*, 2007). Nevertheless, the inaccurate representation of clouds, especially the convective systems, can be also considered as another likely cause of

the disagreement as compared to surface observations (Xia *et al.*, 2006; Wild and Schmucki, 2011; Enriquez-Alonso *et al.*, 2015).

The CV of the annually averaged observed series (Table S1) is low (less than 5%), indicating a weak inter-annual variability of the mean incident global radiation in line with the observed CV in sunshine duration series in the IP

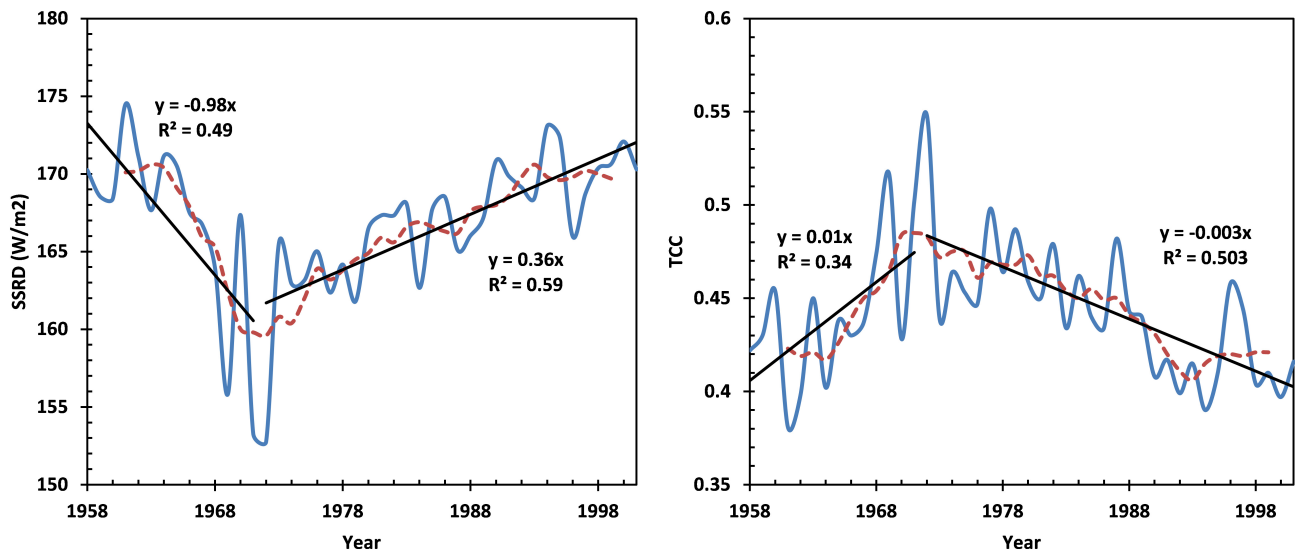


Figure 9. Temporal evolution of the annual mean values of the SSRD and of the TCC, over the whole IP, from ERA-40 data. Red dashed line is the five-year centred moving average. Black solid lines denote linear trends for two periods.

(Gil *et al.*, 2015). The mean annual values of the CV are slightly higher for observations than reanalysis products as these products are based on radiative transfer model computations and not on radiation measurements contributing to smoothing the data series.

3.3. Trends of the SSRD for Portugal and Spain from observations, ERA-40 and NCEP/NCAR data

The least square linear method was applied to the Portugal annual series (see Table 2), and the results indicate that for the whole period only two of the five stations studied (Évora and Faro) show a significant linear trend, whose confirmation was provided by the MK test (Z_{MK} equal to 3.7 and 2.9, respectively). The result shows that in the 1964–1989 period, the trends are relatively strong with an increase in radiation of about $0.9 \text{ W m}^{-2} \text{ year}^{-1}$ in Évora and $0.7 \text{ W m}^{-2} \text{ year}^{-1}$ in Faro. In the other stations, the trends are not statistically significant, as confirmed by the MK test. It is worth mentioning that Évora and Faro show rates of increase in the SSRD comparable with the nearest stations in Spain (Caceres and Malaga), as shown in Table 5 of Sanchez-Lorenzo *et al.* (2013a).

Figure 6 shows the anomaly means of annual SSRD over Portugal and Spain from observations (mean series), ERA-40 and NCEP/NCAR data. The anomaly series are expressed as differences relative to a common period for Portugal (1964–1986) and Spain (1985–2001). In Portugal, ERA-40 and NCEP/NCAR reanalysis replicate the general features of observations. ERA-40 captures the dimming period better than NCEP/NCAR but both transition from dimming to brightening in the early 1970s (see Figure 6). Relative to Spain's annual anomalies (1985–2001), ERA-40 and NCEP/NCAR show a general positive trend as the ground-based observations. Table 4 shows results for linear trends for different periods. For Portugal, signals are similar in all periods (except for the 1978–1986 period in NCEP/NCAR), although

the magnitude of the trends presents slight differences between ground-based stations and reanalysis products as well as the turning year of the dimming/brightening periods. In the case of observational Spanish datasets, only one period (1985–2001) is considered.

Linear regression applied to Portugal over the 1964–1986 period is not statistically significant, as shown by the MK test (see Table 4). For subdivided periods, linear trends show significant values for Portugal, with $-0.5 \text{ W m}^{-2} \text{ year}^{-1}$ for the dimming (1964–1977) period and $-1.1 \text{ W m}^{-2} \text{ year}^{-1}$ for the brightening (1978–1986) period, taking into account a 90% level of confidence. ERA-40 data for the same locations show only a decreasing trend over the 1964–1977 period but with approximately one half of that presented in Portugal and non-significantly for Spain. Results show that NCEP in Spain presents a trend of the same magnitude of observational series ($0.4 \text{ W m}^{-2} \text{ year}^{-1}$), both with a high significance level (above 90%). For detailed SSRD trends over Spanish stations (1985–2001), see analysis in paper of Sanchez-Lorenzo *et al.* (2013a) who found a significant positive trend of around 4 W m^{-2} per decade.

Overall, the decadal changes of the reanalysis products fairly agree with the observations, especially for ERA-40, in contrast to literature for other regions of the world. The comparison between ERA-40 and observations of the SSRD shows a fairly good agreement in the analysed period, especially on a monthly basis, where r values are relatively high. Results obtained from NCEP/NCAR reanalysis have a tendency to be higher than ground-based stations and ERA-40 reanalysis, as seen in biases and decadal changes of radiation shown previously.

The present study suggests that the ERA-40 data may be used in order to study the climatology and evolution of the surface solar radiation and clouds over the regions where aerosol concentrations have not changed significantly.

Results obtained with NCEP/NCAR reanalysis are poorer when compared with observational data.

4. Assessing the SSRD and TCC in the IP from ERA-40 reanalysis data

In this section, the variability and trends of the SSRD and TCC over the IP using ERA-40 reanalysis data from the ECMWF are examined and discussed. Monthly means of SSRD and TCC for the entire period are computed and analysed. The relation between the inter-annual SSRD over the IP and TCC is also analysed.

4.1. General features of the SSRD and TCC climatology

The ERA-40 data was used to create a climatology of the surface solar radiation for the IP. Figure 7 presents the spatial averages of the SSRD and TCC from ERA-40 (1957–2002). As expected, the averaged SSRD presents a latitudinal gradient showing higher values at lower latitudes and lower values at higher latitudes. On the other hand, the mean TCC is larger for higher latitudes. In this period, the mean SSRD ranged from a minimum of 135 W m^{-2} in the northern part of the IP to a maximum of 180 W m^{-2} in the south. The TCC fields shows an opposite spatial pattern with respect to SSRD field. In addition to the latitudinal gradients, Figure 7 also shows longitudinal variations, mainly over the Mediterranean region, with a decrease of the SSRD. A relative maximum of the SSRD in the southern IP is observed, covering the Algarve (Portugal) and Andalusia (Spain). The longitudinal gradient is more intense near the Portuguese West coast. The relation between the SSRD and TCC was investigated in more depth for the period considered.

The IP annual mean values of the SSRD plotted as a function of the corresponding IP mean TCC values clearly illustrates that the SSRD and TCC are negatively correlated with a high coefficient of determination ($R^2 > 0.8$), as shown in Figure S2. This result reveals a strong dependence of clouds on radiation in the ERA-40 and NCEP/NCAR reanalysis. This finding would be expected as the annual aerosol field is fixed, and so only the clouds and the water vapor may have a direct impact on the SSRD.

The spatial distribution of the mean and standard deviation of the SSRD for 2 months (January/July) associated with two different seasons (winter/summer) were computed. Figure 8 depicts the results obtained. In January, the SSRD ranges from about 40 W m^{-2} in the north to more than 80 W m^{-2} in the Murcia region, southeast of Spain. In July, the mean SSRD values are almost four times higher, reaching values close to 300 W m^{-2} in a wide region, including Alentejo and Algarve (Portugal) as well as Estremadura and Andalusia (Spain).

The variability (standard deviation) of the SSRD is larger in January over the southern and central regions of Portugal and Spain, particularly in Extremadura and Andalusia, and lower in the same regions in the summer months. The lower absolute variability observed in the northern part of the IP (Galicia, Asturias, País Vasco) in January

Table 5. Mean, standard deviation (σ), slope (b), R^2 and time series trend obtained from the by the MK test for the SW and TCC in the IP.

	Period	\bar{X}	σ	b	R^2	$Z_{\text{MK}} (\alpha=0.05)$
SSRD	1958–2001	166.9	4.6	0.1	0.1	1.5
	1958–1971	166.9	5.8	−0.97	0.5	−3.0
	1972–2001	166.9	4.1	0.36	0.6	4.7
TCC	1958–2001	0.44	0.0	−0.0	−0.0	−1.6
	1958–1971	0.44	0.0	0.0	0.3	1.8
	1972–2001	0.44	0.0	−0.0	0.5	−4.1

Bold Z_{MK} index means significant trend. In parenthesis is presented the α level of confidence.

is in agreement with the lower values of the SSRD in the region. In winter months, variability in precipitation (clouds) is usually associated to variability in the pathway of the frontal systems, which arise from the Atlantic Ocean (Trigo, 2006; Fragoso *et al.*, 2010; among others).

4.2. Trend analysis of the SSRD and TCC

Figure 9 shows the time series of the spatially averaged annual SSRD and TCC in the IP from 1958 to 2001 and gives a general frame of the evolution of these two quantities in the region. The annual time series of the SSRD and TCC reveal non-statistically significant trends in ERA-40 over the IP for the 1958–2001 period as shown in Table 5 (low values of R^2).

The spatially averaged ERA-40 SSRD mean values with a five-year-centred moving average show two distinct periods for the IP (Figure 9): a decrease of the SSRD in the beginning of the seventies (hereafter referred to as the ERA-40 dimming period) followed by a slight increase up to the end of the time series (hereafter referred to as the ERA-40 brightening period). In contrast, the TCC shows an opposite behavior with a decrease after 1971. Figure 9 allows identifying a maximum of the SSRD over the IP in 1961 with a value of about 175 W m^{-2} and a minimum in 1972 (153 W m^{-2}). With respect to the TCC, an opposite behavior is observed, as referred before, with the maximum obtained in 1972.

According to these results, trends for two separate periods were computed (before and after 1971) and are presented in Figure 9 and Table 5. The annual evolution of the SSRD series shows a statistically significant trend for both periods. In the first period, the SSRD shows a linear decrease of $\sim 1 \text{ W m}^{-2} \text{ year}^{-1}$ with a statistically significant Z_{MK} . In the second period, a slight increase of the radiation is visible, with a slope of $\sim 0.4 \text{ W m}^{-2} \text{ year}^{-1}$ and also with significant Z_{MK} at 95 % level of confidence. An opposite pattern is noticed for the TCC with a significant linear trend only in the second period.

Results from the sequential MK test analysis (Figure 10) show that in the first period (1958–1971), there is a decrease of the SSRD, which started around the late 60s (~ 1967), turning significant in the following year. This result is also consistent with the analysis conducted for the mean of five observational series in Portugal (Section 3).

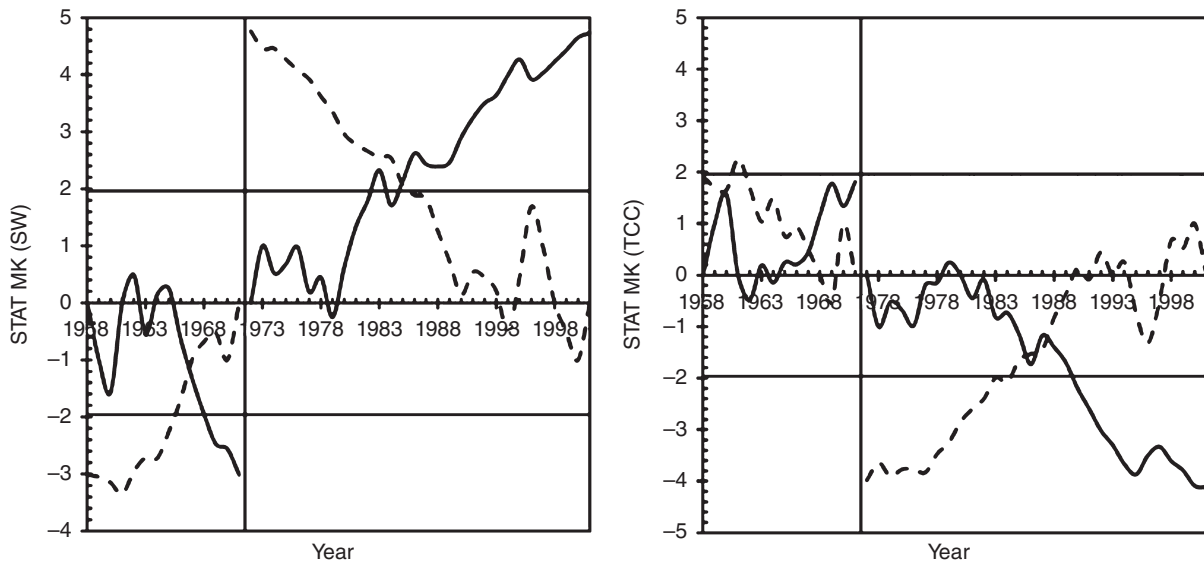


Figure 10. Sequential MK applied to the IP data for the SSRD (a) and TCC (b) divided in two periods (1958–1971) and (1972–2001). The forward series is the solid line and backward series is the dashed line.

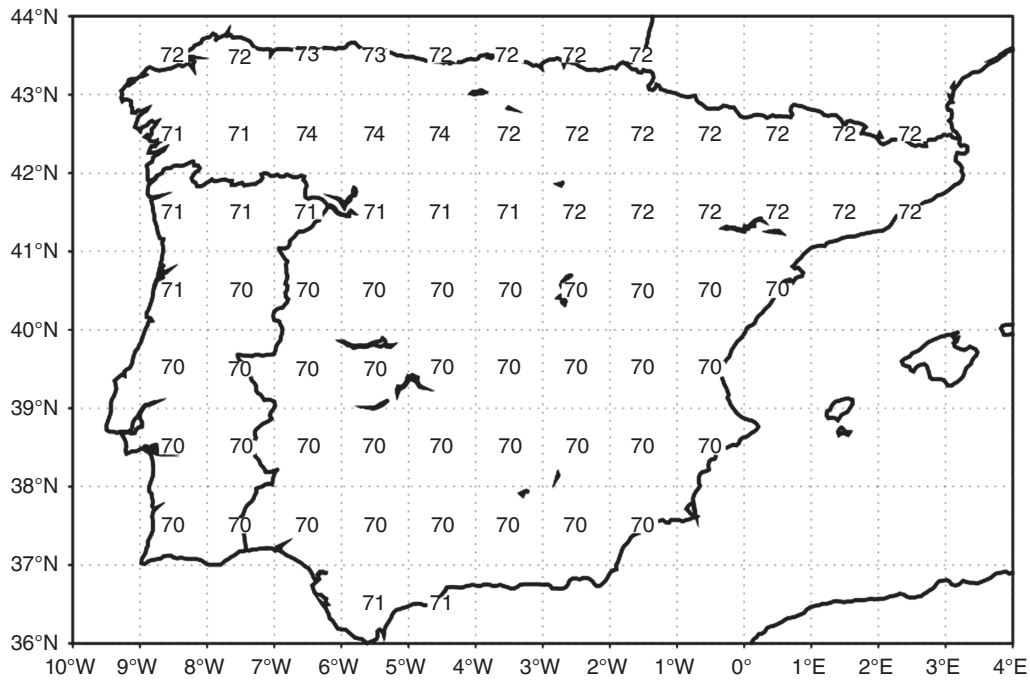


Figure 11. Dimming/brightening transition year computed from ERA-40 SSRD data-set on a 1° × 1° grid over IP.

For the TCC, an opposite behavior is observed with an increase that began in the same year as the SSRD increase but without a statistically significant trend, although positive. In the second period (1972–2001), there is an opposite behavior, with the SSRD presenting a significant statistical increase after 1985, while the TCC decreases for the same year (see Figure 10 and Table 5). These results show that the dimming/brightening phenomena is present in the ECMWF ERA-40 dataset over the IP but that the transition occurred earlier than revealed by the majority of global or regional studies (e.g. Wild *et al.*, 2005; Wild and Schmucki, 2011). It is possible to look at the dimming/brightening on a regional scale. Thus, the IP

was divided into small areas (1° × 1°), and in each of these, a five-year-centred moving average was applied in order to compute the inflection point (minimum value of the centred moving average). The transition year, computed as the minimum of the centred moving average shows a latitudinal gradient (Figure 11), which suggests that the ERA-40 dimming period finished in 1970 in the south and centre IP and a few years later (1973/1974) in the north, 1971 being the average year for the whole Peninsula.

The fact that ERA-40 does not consider the evolution of the aerosol concentration (Uppala *et al.*, 2005) may explain, at least partially, the anticipation of the inflection point in the reanalysis as compared to studies based

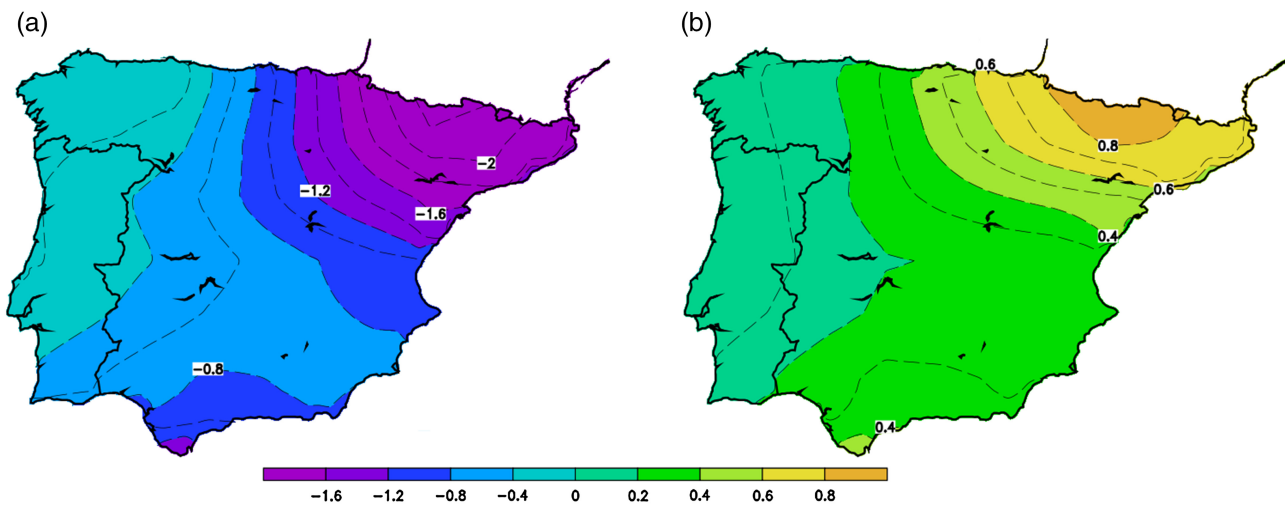


Figure 12. Spatial distribution of linear trends in SSRD for 1957–1971 (a) and 1972–2001 (b) periods.

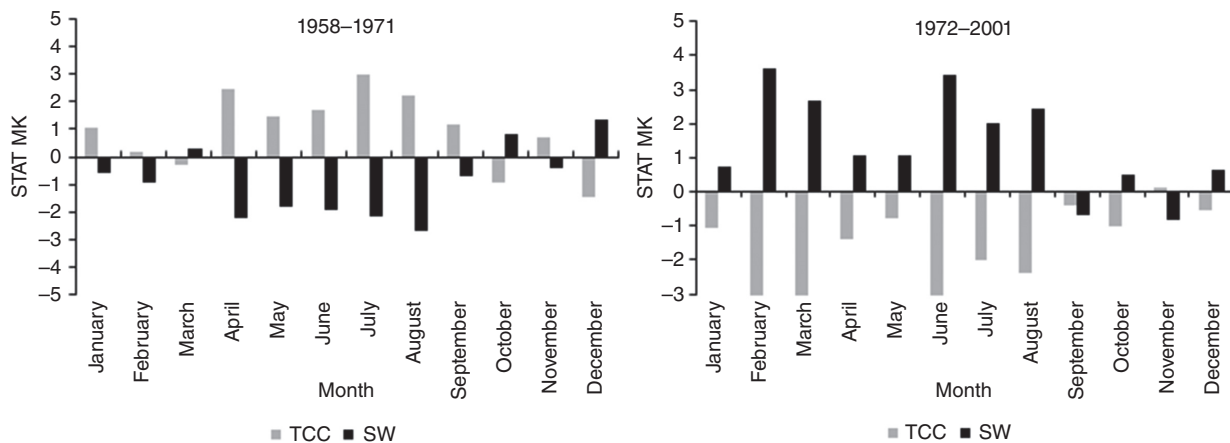


Figure 13. Monthly mean trends in ERA-40 data-set. Results from MK test for the SSRD and TCC over IP.

on ground observations. Note that the transition years in the ERA-40 dataset are consistent with observations in Portuguese stations located in low industrialized regions (Faro and Évora), as shown before (see previous section).

These results show that part of the dimming/brightening phenomena in the IP must be related to decadal changes in the cloud radiative effects and not only to changes in the aerosol loading, especially over south regions where brightening arises 5–10 years earlier than shown in literature (Wild *et al.*, 2005), with a gradient that increases from southwest to northeast.

The SSRD linear trends were computed for the IP in both the ERA-40 dimming (1958–1971) and brightening periods (1972–2001). Figure 12 shows the spatial distribution of the linear regression trends over the IP. For both periods, the pattern of the SSRD trends shows a longitudinal gradient with an increase in the northeast direction. In the first period (1958–1971), trends are always negative with the highest values ($\sim -1.8 \text{ W m}^{-2} \text{ year}^{-1}$) observed in Northeastern Spain, provinces of Navarra, Aragon and Catalonia. For Portugal, the maximum negative trend ($-1 \text{ W m}^{-2} \text{ year}^{-1}$) is found over the south (Alentejo and Algarve). Relative to the second period (1972–2001),

linear trend values are always positive for the entire IP, with a maximum of $+1 \text{ W m}^{-2} \text{ year}^{-1}$ over the same region, while in the first period, major negative trends were found (Northeast region). Although the period of the observational series ‘break’ in different years, there is a tendency to underestimate the trend of the brightening in the reanalysis product as compared to the ground-based observations, with rates below the $4\text{--}6 \text{ W m}^{-2}$ per decade reported in this study and in Sanchez-Lorenzo *et al.* (2013a) and in line with the results of Wild and Schmucki (2011). Equally, it is worth noting that during the dimming period, and especially for the ERA-40, there is a tendency to overestimate the rates of decrease as compared to surface observations, in contrast to Wild and Schmucki (2011).

The monthly mean area-averaged trends in the IP for the SSRD and TCC were computed for both periods and are presented in Figure 13. The results for the first period show that there is a clear decrease of radiation in 75% of the months. The maximum (negative) value of Z_{MK} is reached in August, although with two other months with negative Z_{MK} statistical significance (April and July). In the case of the TCC, the MK test proved to be statistically significant

Table 6. The MK test statistical analysis of the monthly averaged variability in the IP in various periods of study.

Period	Parameter	January	February	March	April	May	June	July	August	September	October	November	December
1958–1971	SSRD	–	–	+	–	–	–	–	–	–	+	–	+
	TCC	+	+	–	+	+	+	+	+	+	–	+	–
1972–2001	SSRD	+	+	+	+	+	+	+	+	–	+	–	+
	TCC	–	–	–	–	–	–	–	–	–	–	+	–

The light grey indicates the existence of trends with a confidence level of 95%.

for the months of April, July and August. However, results show an opposite behaviour relative to the SSRD, with an increase in all months with the exception of March, October and December.

In the second period, an increase in the SSRD (except in September and November) and a decrease in the TCC (except for September) is observed for both parameters and for almost all the months. Table 6 summarizes the results of the monthly tendencies where the grey colour indicates the existence of a statistically significant trend, and the sign indicates positive (+) or negative (–) trends.

As expected, there are opposite trends in both parameters, especially visible for spring and summer periods. The MK test shows an increase of the SSRD in March, in both periods, statistically significant in the first period, which is consistent with that described by Miranda *et al.* (2006).

5. Conclusions

Both downward SSRD and TCC variabilities were studied in the IP based on the ERA-40, NCEP/NCAR reanalysis data and global radiation data for five Portuguese stations obtained from the WRDC and IPMA and processed in this study, and 13 Spanish series available from Sanchez-Lorenzo *et al.* (2013a) were also used.

The SSRD mean series in Portugal show two distinct periods of decrease and increase during the study period, known as the dimming and brightening periods in the literature, although with an earlier turning year (around 5 years) than that described in the literature, in particular over the south of Portugal. The observational data reveal an increasing trend of global radiation in the stations located in the south of Portugal, without a pronounced decrease before the 1980s, in the period 1964–1986.

The least square linear method shows a statistically significant increase in the SSRD of $1 \text{ W m}^{-2} \text{ year}^{-1}$ in the study period for Évora and Faro. This behaviour can mainly be explained by the inter-annual variability of clouds and respective synoptic patterns over the North Atlantic Ocean. Overall, the observations suggest that the decadal evolution of the SSRD may be influenced by local causes associated to human activities, particularly the emission of aerosols, as well as cloud changes.

The ERA-40 database underestimates the SSRD in comparison to the observations for Portugal and Spain, whereas the NCEP/NCAR overestimated the latter. The correlation coefficients (r) found between the ground-based stations for Portugal and Spain obtained from the nearest ERA-40 and NCEP/NCAR grid data points are relatively high for

the monthly series. The correlation coefficient values are specifically above 0.7, with the highest values obtained during winter and autumn seasons.

From reanalysis and for the IP, it seems that the ERA-40 captures the decadal variability observed in ground-based SSRD records better than the NCEP/NCAR. The time evolution of the ERA-40 SSRD values for the IP shows two distinct periods: a decrease of the SSRD at the beginning of the 70s (ERA-40 dimming period) followed by a slight increase up to the end of the time series (ERA-40 brightening period), with significant linear trends of $\sim -1 \text{ W m}^{-2} \text{ year}^{-1}$ and $+0.4 \text{ W m}^{-2} \text{ year}^{-1}$, respectively. For both periods, it is possible to see a longitudinal gradient toward the northeast direction. The TCC shows an opposite behaviour.

The SSRD and TCC are negatively correlated with a fairly high coefficient of determination ($R^2 > 0.8$). This finding would be expected as the annual aerosol field is fixed (Uppala *et al.*, 2005). Results show that part of the dimming/brightening phenomena in the IP must be related to decadal changes in the cloud radiative effects and not only to changes in the aerosol loading, especially over southern regions where brightening arises approximately 5 years earlier than reported in literature (Wild *et al.*, 2005).

The ERA-40 reveals a reasonable ability to simulate the radiation, in particular on a monthly basis, considering the uncertainty in the observational data, the problem of fixed aerosols in the reanalysis data and its spatial resolution. It was thus possible to obtain useful, low-resolution climatology data of the surface global solar radiation over IP based on ERA-40 reanalysis.

Acknowledgement

The authors acknowledge the funding provided by ICT, under contract with FCT (the Portuguese Science and Technology Foundation) and by the FEDER (Programa Operacional Factores de Competitividade COMPETE) and FCT in the framework of project FCOMP-01-0124-FEDER-041840 (EXPL/GEO-MET/1422/2013). Arturo Sanchez-Lorenzo was supported by a postdoctoral fellowship JCI-2012-12508 and the projects CGL2014-55976-R, CGL2014-52135-C3-01-R from the Spanish Ministry of Economy and Competitiveness. The authors would also like to thank the ECMWF for providing ERA-40 data. NCEP Reanalysis data was provided by the NOAA/OAR/ESRL through the website at <http://www.esrl.noaa.gov/psd>. Authors would also like to thank to AEMET (Spanish Agencia Estatal de

Meteorologia) and IPMA (Instituto Português do Mar e da Atmosfera) for providing ground-based data.

Supporting Information

The following supporting information is available as part of the online article:

Table S1. Descriptive statistics of the annual mean of the SSRD for observed and reanalysis data over Portugal and Spain.

Figure S1. Correlation coefficients (dots) and bias (bars) between the monthly mean series of observed SSRD at selected meteorological stations (Portugal and Spain) and reanalysis products nearest grid point.

Figure S2. SSRD radiation *versus* TCC spatially averaged over IP for the ERA-40 (a) and NCEP/NCAR (b). SSRD in $W m^{-2}$. TCC NCEP/NCAR data in percentage.

References

- Alados-Arboledas L, Lyamani H, Olmo FJ. 2003. Aerosol size properties at Armilla, Granada (Spain). *Q. J. R. Meteorol. Soc.* **129**(590): 1395–1414, doi: 10.1256/qj.01.207.
- Albrecht B. 1989. Aerosols, cloud microphysics, and fractional cloudiness. *Science* **245**: 1227–1230, doi: 10.1126/science.245.4923.1227.
- Alexandersson H. 1986. A homogeneity test applied to precipitation data. *J. Climatol.* **6**: 661–675.
- Alpert P, Kishcha P. 2008. Quantification of the effect of urbanization on solar dimming. *Geophys. Res. Lett.* **35**: L08801, doi: 10.1029/2007GL033012.
- Alpert P, Kishcha P, Kaufman YJ, Schwarzbard R. 2005. Global dimming or local dimming?: effect of urbanization on sunlight availability. *Geophys. Res. Lett.* **32**: L17802, doi: 10.1029/2005GL023320.
- Antón M, Valenzuela A, Cazorla A, Gil JE, Fernández-Gálvez J, Lyamani H, Foyo-Moreno I, Olmo FJ, Alados-Arboledas L. 2012. Global and diffuse shortwave irradiance during a strong desert dust episode at Granada (Spain). *Atmos. Res.* **118**: 232–239, doi: 10.1016/j.atmosres.2012.07.007.
- Augustine JA, Dutton EG. 2013. Variability of the surface radiation budget over the United States from 1996 through 2011 from high-quality measurements. *J. Geophys. Res. Atmos.* **118**: 43–53, doi: 10.1029/2012JD018551.
- Betts AK, Zhao M, Dirmeyer PA, Beljaars ACM. 2006. Comparison of ERA-40 and NCEP/DOE near-surface data sets with other ISLSCP-II data sets. *J. Geophys. Res.* **111**: D22S04, doi: 10.1029/2006JD007174.
- Buishand T. 1982. Some methods for testing the homogeneity of rainfall records. *J. Hydrol.* **58**: 11–27.
- Chiacchio M, Wild M. 2010. Influence of NAO and clouds on long-term seasonal variations of surface solar radiation in Europe. *J. Geophys. Res.* **115**(D00D22): 1–17, doi: 10.1029/2009JD012182.
- Chiacchio M, Ewen T, Wild M, Arabini E. 2010. Influence of climate shifts on decadal variations of surface solar radiation in Alaska. *J. Geophys. Res.* **115**(D00D21): 1–19, doi: 10.1029/2009JD012533.
- Cislaghi M, De Michele C, Ghezzi A, Rosso R. 2005. Statistical assessment of trends and oscillations in rainfall dynamics. Analysis of long daily Italian series. *Atmos. Res.* **77**(1–4): 188–202, doi: 10.1016/j.atmosres.2004.12.014.
- Cravidão F, Matos MA. 1990. A população portuguesa dos anos 60 ao final do século xx: o envelhecimento acelerado. In *Cadernos de Geografia* n. 9. Universidade de Coimbra, Coimbra, 35–48.
- Enriquez-Alonso A, Sanchez-Lorenzo A, Calbó J, González JA, Norris JR. 2015. Cloud cover climatologies in the Mediterranean obtained from satellites, surface observations, reanalyses, and CMIP5 simulations: validation and future scenarios. *Clim. Dyn.* 1–21, doi: 10.1007/s00382-015-2834-4.
- Fouquart Y, Bonnel B. 1980. Computation of solar heating of the Earth's atmosphere: a new parameterization. *Beitr. Phys. Atmos.* **53**: 35–62.
- Fragoso M, Trigo RM, Zêzere JL, Valente MA. 2010. The exceptional rainfall event in Lisbon on 18 February 2008. *Weather* **65**(2): 31–35, doi: 10.1002/wea.513.
- Gil V, Gaertner MA, Sanchez E, Gallardo C, Hagel E, Tejada C, Castro M. 2015. Analysis of interannual variability of sunshine hours and precipitation over Peninsular Spain. *Renew. Energy* **83**: 680–689, doi: 10.1016/j.renene.2015.05.001.
- Hakuba MZ, Sanchez-Lorenzo A, Folini D, Wild M. 2013. Testing the homogeneity of short-term surface solar radiation series in Europe. *AIP Conference Proceedings* **1531**: 700–703, doi: 10.1063/1.4804866.
- Hakuba MZ, Folini D, Sanchez-Lorenzo A, Wild M. 2014. Spatial representativeness of ground-based solar radiation measurements – Extension to the full Meteosat disk. *J. Geophys. Res. Atmos.* **119**: 11, 760–11, 771, doi: 10.1002/2014JD021946.
- Hammer A, Heinemann D, Hoyer C, Kuhlemann R, Lorenz E, Müller R, Beyer HG. 2003. Solar energy assessment using remote sensing technologies. *Remote Sens. Environ.* **86**: 423–432.
- Hurrell JW. 1995. Decadal trends in the North Atlantic Oscillation: regional temperatures and precipitation. *Science* **269**: 676–679.
- Hurrell JW. 1996. Influence of variations in extratropical wintertime teleconnections on Northern Hemisphere temperatures. *Geophys. Res. Lett.* **23**(6): 665–668.
- Kalnay E, Kanamitsu M, Kistler R, Collins W, Deaven D, Gandin L, Iredell M, Saha S, White G, Woollen J, Zhu Y, Chelliah M, Ebisuzaki W, Higgins W, Janowiak J, Mo KC, Ropelewski C, Wang J, Leetmaa A, Reynolds R, Jenne R, Joseph D. 1996. The NCEP/NCAR 40-year reanalyses projects. *Bull. Am. Meteorol. Soc.* **77**: 437–471.
- Kaurola J, Lindfors A, Lakkala K, Hansen G, Josefsson W, Vuilleumier L, Feister U, Slaper H. 2010. On the usability of the ERA-40 reanalysis in the estimation of past surface UV radiation over Europe. *J. Geophys. Res.* **115**: D24107, doi: 10.1029/2010JD013810.
- Khalilq MN, Ouarda TBMJ. 2007. Short communication on the critical values of the standard normal homogeneity test (SNHT). *Int. J. Climatol.* **27**(5): 681–687.
- Leite F, Gonçalves A, Lourenço L. 2014. Grandes Incêndios florestais na década de 60 do Século XX, em Portugal Continental. *Territorium: Revista Portuguesa de riscos, prevenção e segurança* **21**: 189–195.
- Liepert BG. 2002. Observed reductions of surface solar radiation at sites in the United States and worldwide from 1961 to 1990. *Geophys. Res. Lett.* **29**(10): 1421, doi: 10.1029/2002GL014910.
- Liepert B, Tegen I. 2002. Multi-decadal solar radiation trends in the United States and Germany and direct tropospheric aerosol forcing. *J. Geophys. Res.* **107**(12): 4153, doi: 10.1029/2001JD000760.
- Liley JB. 2009. New Zealand dimming and brightening. *J. Geophys. Res.* **114**: D00D10, doi: 10.1029/2008JD01140.
- Liu C, Liu X, Zheng H, Zeng Y. 2010. Change of the solar radiation and its causes in the Haihe River Basin and surrounding areas. *J. Geogr. Sci.* **20**(4): 569–580, doi: 10.1007/s11442-010-0569-z.
- Lohmann U, Feichter J. 2005. Global indirect aerosol effects: a review. *Atmos. Chem. Phys.* **5**: 715–737, doi: 10.5194/acp-5-715-2005.
- Manara V, Beltrano MC, Brunetti M, Mauderi M, Sanchez-Lorenzo A, Simolo C, Sorrenti S. 2015. Sunshine duration variability and trends in Italy from homogenized instrumental time series (1936–2013). *J. Geophys. Res. Atmos.* **120**: 3622–3641, doi: 10.1002/2014JD022560.
- Mann HB. 1945. *Econometrica*. *Econm. Soc.* **13**(3): 245–259.
- Mateos D, Sanchez-Lorenzo A, Antón M, Cachorro VE, Calbó J, Costa MJ, Torres B, Wild M. 2014. Quantifying the respective roles of aerosols and clouds in the strong brightening since the early 2000s over the Iberian Peninsula. *J. Geophys. Res. Atmos.* **119**(10): 10382–10393, doi: 10.1002/2014JD022076.
- Miranda P, Valente M, Tomé A, Trigo R, Coelho M, Aguiar A, Azevedo E. 2006. O clima de Portugal nos séculos XX e XXI. In *Alterações Climáticas em Portugal – Cenários, Impactos e Medidas de Adaptação – Projecto SIAM_II*, Santos FD, Miranda P (eds). Gradiva, Lisboa, Portugal, 47–113.
- Morozova AL, Valente MA. 2012. Homogenization of Portuguese long-term temperature data series: Lisbon, Coimbra and Porto. *Earth Syst. Sci. Data* **4**: 187–213, doi: 10.5194/essd-4-187-2012.
- Norris JR, Wild M. 2007. Trends in aerosol radiative effects over Europe inferred from observed cloud cover, solar “dimming,” and solar “brightening”. *J. Geophys. Res.* **112**: D08214, doi: 10.1029/2006JD007794.
- Obot NI, Chendo MAC, Udo SO, Ewona IO. 2010. Evaluation of rainfall trends in Nigeria for 30 years (1978–2007). *Int. J. Phys. Sci.* **5**(14): 2217–2222.
- Obregón MA, Pereira S, Wagner F, Serrano A, Cancillo ML, Silva AM. 2012. Regional differences of column aerosol parameters in western Iberian Peninsula. *Atmos. Environ.* **62**: 208–219, doi: 10.1016/j.atmosenv.2012.08.016.

- Obrégón MA, Pereira S, Salgueiro V, Costa MJ, Silva AM, Serrano A, Bortoli D. 2015. Aerosol radiative effects during two desert dust events in August 2012 over the Southwestern Iberian Peninsula. *Atmos. Res.* **153**: 404–415, doi: 10.1016/j.atmosres.2014.10.007.
- Ohmura A, Lang H. 1989. Secular variation of global radiation over Europe. In *Current Problems in Atmospheric Radiation*, Lenoble J, Geleyn JF (eds). Deepak: Hampton, VA, 298–301.
- Pettitt AN. 1979. A non-parametric approach to the change-point problem. *J. R. Stat. Soc. Ser. C: Appl. Stat.* **28**: 126–135.
- Pozo-Vázquez D, Tovar-Pescador J, Gámiz-Fortis SR, Esteban-Parra MJ, Castro-Díez Y. 2004. NAO and solar radiation variability in the European North Atlantic region. *Geophys. Res. Lett.* **31**: L05201, doi: 10.1029/2003GL018502.
- Qian Y, Wang W, Leung LR, Kaiser DP. 2007. Variability of solar radiation under cloud-free skies in China: the role of aerosols. *Geophys. Res. Lett.* **34**: L12804, doi: 10.1029/2006GL028800.
- Russak V. 2009. Changes in solar radiation and their influence on temperature trend in Estonia (1955–2007). *J. Geophys. Res.* **114**: D00D01, doi: 10.1029/2008JD010613.
- Sanchez-Lorenzo A, Calbó J, Brunetti M, Deser C. 2009. Dimming/brightening over the Iberian Peninsula: trends in sunshine duration and cloud cover and their relations with atmospheric circulation. *J. Geophys. Res.* **114**: D00D09, doi: 10.1029/2008JD011394.
- Sanchez-Lorenzo A, Calbó J, Wild M. 2013a. Global and diffuse solar radiation in Spain: building a homogeneous dataset and assessing their trends. *Glob. Planet. Change* **100**: 343–352.
- Sanchez-Lorenzo A, Wild M, Trentmann J. 2013b. Validation and stability assessment of the monthly mean CM SAF surface solar radiation dataset over Europe against a homogenized surface dataset (1983–2005). *Remote Sens. Environ.* **134**: 355–366.
- Sanchez-Lorenzo A, Wild M, Brunetti M, Guijarro JA, Hakuba M, Calbó J, Mystakidis S, Bartok B. 2015. Reassessment and update of long-term trends in downward surface shortwave radiation over Europe (1939–2012). *J. Geophys. Res. Atmos.* **120**: 9555–9569, doi: 10.1002/2015JD023321.
- Silva VP, Silva RA, Cavalcanti EP, Braga CC, Azevedo PV, Singh VP, Pereira ERR. 2010. Trends in solar radiation in NCEP/NCAR database and measurements in northeastern Brazil. *Sol. Energy* **84**: 1852–1862, doi: 10.1016/j.solener.2010.07.011.
- Sneyers R. 1975. Sur l'analyse statistique des series d'observations. Note Technique 143, OMM, Geneva, 192 pp.
- Stanhill G, Cohen G. 2001. Global dimming: a review of the evidence for a widespread and significant reduction in global reduction with discussion of its probable causes on possible agriculture consequences. *Agric. For. Meteorol.* **107**: 255–278, doi: 10.1016/S0168-1923(00)00241-0.
- Stanhill G, Moreshet S. 1992. Global radiation climate changes: the world network. *Clim. Change* **21**: 57–75, doi: 10.1007/BF00143253.
- Stjern CW, Kristjánsson JE, Hansen AW. 2009. Global dimming and global brightening – an analysis of surface radiation and cloud cover data in northern Europe. *Int. J. Climatol.* **29**: 643–653, doi: 10.1002/joc.1735.
- Toledano C, Cachorro VE, Berjon A, de Frutos AM, Sorribas M, de la Morena BA, Goloub P. 2007. Aerosol optical depth and Ångström exponent climatology at El Arenosillo AERONET site (Huelva, Spain). *Q. J. R. Meteorol. Soc.* **133**: 795–807, doi: 10.1002/qj.54.
- Träger-Chatterjee C, Müller RW, Trentmann J, Bendix J. 2010. Evaluation of ERA-40 and ERA-interim re-analysis incoming surface shortwave radiation datasets with mesoscale remote sensing data. *Meteorol. Z.* **19**(6): 631–640, doi: 10.1127/0941-2948/2010/0466.
- Trigo IF. 2006. Climatology and interannual variability of storm-tracks in the Euro-Atlantic sector: a comparison between ERA-40 and NCEP/NCAR reanalyses. *Clim. Dyn.* **26**: 127–143.
- Trigo RM, Osborn TJ, Corte-Real JM. 2002. The North Atlantic Oscillation influence on Europe: climate impacts and associated physical mechanisms. *Clim. Res.* **20**: 9–17.
- Twomey SA, Piepgrass M, Wolfe TL. 1984. An assessment of the impact of pollution on global cloud albedo. *Tellus* **36B**: 356–366.
- Uppala SM, Kållberg PW, Simmons AJ, Andrae U, Bechtold VDC, Fiorino M, Gibson JK, Haseler J, Hernandez A, Kelly GA, Li X, Onogi K, Saarinen S, Sokka N, Allan RP, Andersson E, Arpe K, Balmaseda MA, Beljaars ACM, Berg LVD, Bidlot J, Bormann N, Caires S, Chevallier F, Dethof A, Dragosavac M, Fisher M, Fuentes M, Hagemann S, Hólm E, Hoskins BJ, Isaksen I, Janssen PAEM, Jenne R, McNally AP, Mahfouf J-F, Morcrette J-J, Rayner NA, Saunders RW, Simon P, Sterl A, Trenberth KE, Untch A, Vasiljevic D, Viterbo P, Woollen J. 2005. The ERA-40 re-analysis. *Q. J. R. Meteorol. Soc.* **131**: 2961–3012, doi: 10.1256/qj.04.176.
- Valenzuela A, Olmo FJ, Lyamani H, Antón M, Quirantes A, Alados-Arboledas L. 2012. Aerosol radiative forcing during African desert dust events (2005–2010) over Southeastern Spain. *Atmos. Chem. Phys.* **12**: 10331–10351, doi: 10.5194/acp-12-10331-2012.
- Von Neumann J. 1941. Distribution of the ratio of the mean square successive difference to the variance. *Ann. Math. Stat.* **12**: 367–395.
- Wang K, Ma Q, Li Z, Wang J. 2015. Decadal variability of surface incident solar radiation over China: observations, satellite retrievals, and reanalyses. *J. Geophys. Res. Atmos.* **120**: 6500–6514, doi: 10.1002/2015JD023420.
- Wijngaard JB, Klein Tank AMG, Können GP. 2003. Homogeneity of 20th century European daily temperature and precipitation series. *Int. J. Climatol.* **23**: 679–692, doi: 10.1002/joc.906.
- Wild M. 2001. Surface and atmospheric radiation budgets as determined in reanalyses. In *IRS2000: Current Problems in Atmospheric Radiation*, Smith WL, Timofeyev YM (eds). A Deepak Publishing: Hampton, VA, 602–605.
- Wild M. 2009. Global dimming and brightening: a review. *J. Geophys. Res.* **114**: D00D16, doi: 10.1029/2008JD011470.
- Wild M. 2010. Introduction to special section on global dimming and brightening. *J. Geophys. Res.* **115**: D00D00, doi: 10.1029/2009JD012841.
- Wild M. 2012. Enlightening global dimming and brightening. *Bull. Am. Meteorol. Soc.* **93**: 27–37, doi: 10.1175/BAMS-D-11-00074.1.
- Wild M, Schmucki E. 2011. Assessment of global dimming and brightening in IPCC-AR4/CMIP3 models and ERA-40. *Clim. Dyn.* **37**: 1671–1688, doi: 10.1007/s00382-010-0939-3.
- Wild M, Gilgen H, Roesch A, Ohmura A, Long CN, Dutton EG, Forgan B, Kallis A, Russak V, Tsvetkov A. 2005. From dimming to brightening: decadal changes in surface solar radiation. *Science* **308**: 847–850, doi: 10.1126/science.1103215.
- Wild M, Folini D, Henschel F, Fischer N, Müller B. 2015. Projections of long-term changes in solar radiation based on CMIP5 climate models and their influence on energy yields of photovoltaic systems. *Sol. Energy* **16**: 12–24.
- Xia X. 2010. A closer looking at dimming and brightening in China during 1961–2005. *Ann. Geophys.* **28**: 1121–1132, doi: 10.5194/angeo-28-1121-2010.
- Xia XA, Wang PC, Chen HB, Liang F. 2006. Analysis of downwelling surface solar radiation in China from National Centers for Environmental Prediction reanalysis, satellite estimates, and surface observations. *J. Geophys. Res.* **111**: D09103, doi: 10.1029/2005JD006405.
- You Q, Sanchez-Lorenzo A, Wild M, Folini D, Fraedrich K, Ren G, Kang S. 2013. Decadal variation of surface solar radiation in the Tibetan Plateau from observations, reanalysis and model simulations. *Clim. Dyn.* **40**(7–8): 2073–2086, doi: 10.1007/s00382-012-1383-3.
- Yu H, Kaufman YJ, Chin M, Feingold G, Remer LA, Anderson TL, Balkanski Y, Bellouin N, Boucher O, Christopher S, DeCola P, Kahn R, Koch D, Loeb N, Reddy MS, Schulz M, Takemura T, Zhou M. 2006. A review of measurement-based assessments of the aerosol direct radiative effect and forcing. *Atmos. Chem. Phys.* **6**: 613–666, doi: 10.5194/acp-6-613-2006.